Elastic scattering induced by halo nuclei

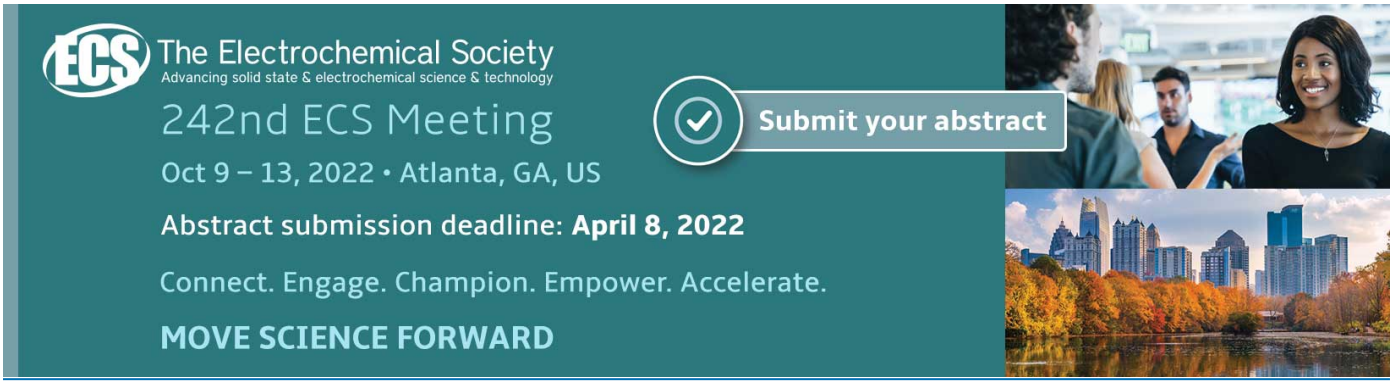

Elastic scattering induced by halo nuclei

A Di Pietro[1], P Figuera[1], M Fisichella[1,2], M Lattuada[1,3] and M Zadro[4]

[1] INFN-Laboratori Nazionali del Sud, via S. Sofia 62, 95125 Catania, Italy.
[2] Centro Siciliano di Fisica Nucleare e Struttura della Materia, Viale A. Doria, 6 Catania Catania 95125 Italy.
[3] Dipartimento di Fisica ed Astronomia, Universitá di Catania, Viale A. Doria, 6 Catania Catania 95125 Italy.
[4] Division of Experimental Physics Ruđer Bošković Institute, Bijenička cesta 54, 10000 Zagreb, Croatia.

E-mail: dipietro@lns.infn.it

Abstract. In this paper an overview of different results concerning elastic scattering in collisions induced by halo nuclei will be given. Due to the very low binding energy of such nuclei, coupling effects with the break-up channel have been found to be very important. Moreover, due to the long tail of the density distribution of halo nuclei and the presence of a large low-lying dipole strength distribution, long range absorption affects the elastic scattering angular distribution. In the paper the main effects responsible for the observed features in the scattering cross-section will be discussed.

1. Introduction

Nuclear halo is a threshold phenomenon arising from the very weak binding of the last one or two valence nucleons which decouples from an inert core that contains all the other nucleons [1]. The core is compact and thus, due to the combination between the short range nuclear force and the weak binding, the valence nucleon(s) can tunnel out into a volume which goes well beyond the nuclear core into the classically-forbidden region. For these reasons, the single-particle wave function of the valence nucleons in halo nuclei has a long tail, which extends mostly outside the potential well.

Since the first observations, a lot of experiments have been performed in order to investigate this peculiar structure also in the attempt to understand how this structure is affecting the reaction process in collisions induced by halo nuclei (see e.g. [2, 3, 4, 5]). Since elastic scattering is a peripheral process, it can be used to probe the tail of the wave function thus allowing to learn about the surface properties of these nuclei.

Elastic scattering was generally considered a simple process where the internal structure of the colliding nuclei has no or little effect on the outcome of the process. Angular distributions are characterized by two regions, divided by the "grazing angle" or "quarter point angle" which separate the illuminated or classically allowed region from the shadow or classically forbidden region. However, the striking shape of the angular distribution asks for attempts to interpret the data in a more complex way in which the explicit inclusion of coupling effects between relative motion and internal degrees of freedom is required.

Due to the low binding energy of halo nuclei, the coupling not only to bound and unbound

excited states but also to the continuum (break-up) is needed (see e.g. [6, 7, 8, 9]).
Elastic scattering experiments involving halo nuclei have been performed at several energies and on targets covering a wide range of masses. These studies have mainly been performed with the 2n-halo ^{6}He nucleus but, more recently, data have appeared in the literature concerning elastic scattering of halo nuclei different than ^{6}He. Many of the measured elastic scattering angular distributions differ deeply from the one induced by the corresponding non-halo isotope. A common feature observed in the low-energy halo-induced elastic scattering, on medium mass and heavy targets, is a reduction of the Coulomb-nuclear interference peak (e.g. [4, 10]) often called in the literature Coulomb "rainbow". The suppression of the Coulomb-nuclear interference seems to be attributed to long range absorption which smooths the surface-jump of the scattering matrix $|S(l)|$. A further consequence of this suppression is a much larger total-reaction (TR) cross-section with respect to the one measured in reactions induced by the corresponding non-halo isotope (e.g. [10, 11]).
From a theoretical point of view, most of the experimental data available in the literature have been analyzed either within the Optical Model (OM) or within the Coupled Channel (CC) formalism. In the OM framework, in order to include the effects of coupling, a Dynamic Polarization Potential (DPP) has been added to the bare potential; the latter has been obtained either phenomenologically or via a double folding procedure. As mentioned above, in collisions induced by halo nuclei, coupling with the continuum is important. Since the coupling with the continuum originates a repulsive DPP (see e.g.[12, 13]), the usual threshold anomaly in the optical potential (OP) [14], which arises from the presence of an attractive DPP, may disappear. A new type of dependence of the OP with the energy, characterized by the absence of the usual threshold anomaly, called in the literature "*breakup threshold anomaly*" (BTA) shows up (see e.g. [15, 16, 17]). Weakly bound halo systems are characterized by a low-lying large dipole strength just above the break-up threshold, it has been found that coupling with this B(E1) strength is important in heavy targets.
In the CC formalism coupling to the continuum is introduced by discretizing the continuum, for each partial wave, from the break-up threshold up to a maximum excitation energy in a finite number of bins evenly spaced in the linear momentum. These type of calculations are called Continuum Discretized Coupled Channel (CDCC) calculations see e.g. [18].
In this paper, an overview of the experimental results present in the literature will be given. In the second section a survey of the elastic scattering results on light targets, obtained both below and well above the barrier, will be presented. In the third section will be presented the results of scattering on medium mass targets and, in section 4, the results that have been obtained on heavy targets.

2. Scattering on light targets

The ^{6}He+^{9}Be elastic scattering has been studied in [19] at E_{lab}=16.8 MeV and in [22] at 16.2 and 21.3 MeV. In [19], an OM analysis was performed using as starting OM parameters the ones from existing ^{6}Li+^{9}Be data and varying the depth of the real and imaginary potential. This analysis did not lead to a good agreement with the data. In [22], in order to investigate the effect of target and projectile excitation, CC calculations were performed where coupling to low-lying rotational states of ^{9}Be and the low-lying 2^+ state in ^{6}He were considered. The agreement with the data improved with respect to the no-coupling case, however a much better agreement with the data, especially at the highest energy, was obtained when coupling to the continuum was included using CDCC calculations. This was also the case for [19]. In order to study the effect of coupling in terms of a DPP, in [22], a trivial local DPP (TLP) was deduced using the prescription of [23]. The extracted real part of the TLP was found to be repulsive at a distance around the sum of the projectile and target radii, whereas the imaginary part has a diffuse tail. These features are similar to the ones found in collisions induced by weakly bound

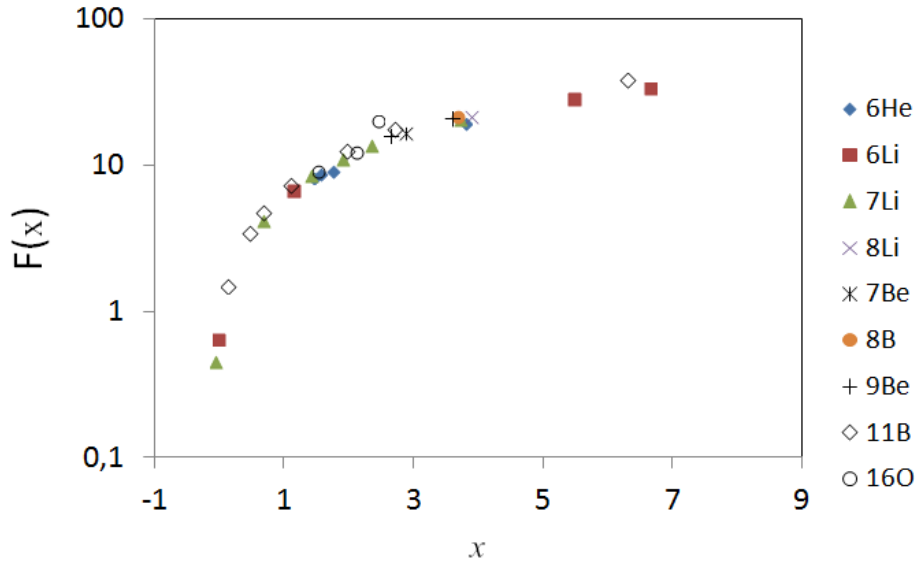

Figure 1. Reduced reaction cross-section for different collisions on ^{12}C targets. Data are from [30] and ref. therein. See text for details.

nuclei and that lead to the occurrence of the BTA, discussed in the introduction.
Contrary to what happens with heavy targets, on light targets the effect of Coulomb break-up is negligible, the effect of coupling on the angular distribution is almost entirely due to nuclear couplings. Another difference that has been observed between light and heavy targets is that, in order to reproduce the data, the inclusion of coupling to the quadrupole 2^+ states in the 2n-α continuum, in the case of ^{6}He, is important while for heavy targets the main effect comes from the coupling with the Coulomb dipole strength [22].

Elastic scattering angular distributions of ^{6}He on ^{6,7}Li and ^{12}C have been reported in [24, 25]. In the analysis of the scattering on ^{6,7}Li targets, global OM potential parameters obtained for the reactions induced by ^{6,7}Li beams were used while, for the scattering on ^{12}C, the potential parameters used were the ones of ^{6}Li+^{12}C at similar energies. Contrary to what found in [19] a good reproduction of the data was obtained in these cases. In order to see possible effects of the halo structure of ^{6}He, the radius of the imaginary potential was increased by 10%. This change produced an overall disagreement with the data. The ^{6}He+^{12}C data were analysed also by Matsumoto et al. [8], using the four-body CDCC approach. A large effect due to the coupling with the four-body break-up is found in these calculations. Moreover, a 15% enhancement of the TR cross-section, with respect to the cross-section of ^{6}Li+^{12}C at a similar energy, is found. In these calculations the Coulomb break-up is neglected.
^{6}He+^{12}C elastic scattering data at much higher energy, 38.3 MeV/nucleon, are reported in [21]. In their analysis OM calculations were performed which required a complex DPP potential, that was added to the double-folding bare potential. The DPP had a repulsive real part in order to account for effects due to the break-up. Four-body CDCC calculations were also performed in [8] which were able to reproduce very well the data once the four body break-up was introduced. Contrary to what found at lower energy , these calculations predict a suppression of the ^{6}He+^{12}C TR cross-section when compared to the ^{6}Li+^{12}C one.
In [32], ^{11}Be+^{12}C scattering data at 49.3 MeV/nucleon were analysed within the OM using as bare potential the one extracted from the ^{10}Be+^{12}C scattering and an analytically derived complex surface DPP which was evaluated from the calculation of the break-up probability.

By assuming an exponential tail for the imaginary surface potential, its diffuseness is directly related to the decay length of the halo wave function. In the case under investigation the obtained diffuseness is 3.2 fm and it depends only on the projectile characteristics and not on the target. A similar diffuseness was in fact obtained in [10] on a different target, as will be discussed in the next section.
In [26] the elastic scattering of ^{6}He on ^{27}Al was measured. The data are rather limited, however the total reaction cross-section was deduced at four energies ranging from 9.5 MeV to 13.4 MeV. The extracted total reaction cross-sections were compared with the ones of stable weakly-bound nuclei (^{6,7}Li and ^{9}Be) and well bound ^{16}O nucleus on the same ^{27}Al target. It was found that, within the errors, the total reaction cross-section of ^{6}He behaves in a similar way as the weakly-bound nuclei and that is larger than for the well bound closed shell ^{16}O.
Elastic scattering of the p-halo ^{8}B nucleus on a ^{12}C target was measured by [30]. CDCC calculations were performed which showed that the effect of break-up coupling for this system is very weak. Moreover in [30], the TR cross-section was deduced and compared with the total reaction cross-section for collisions on the same ^{12}C target induced either by halo (^{6}He,^{8}B), weakly-bound (^{6,7,8}Li, ^{7}Be) and well bound (^{10}Be, ^{11}B, ^{16}O) beams. It was found that, contrary to what concluded in [26], the total reaction cross-section for all these systems follows the same trend. In fig. 1 this comparison is shown. In this case, for matter of comparison, the cross-sections were reduced, in order to eliminate trivial static effects, according to what suggested by [31], where:

$$x = \frac{(E - V_B)}{\hbar\omega}; \tag{1}$$

and

$$F(x) = \frac{2E}{\hbar\omega R^2}\sigma_R; \tag{2}$$

3. Scattering on medium mass targets

As mentioned in the introduction, strong Coulomb coupling effects are expected to affect the elastic scattering angular distribution when the atomic number of the target nucleus (Z_T) is large. As the charge of the target increases, the breakup of the weakly bound projectile is expected to increase as well due to the enhanced importance of the Coulomb break-up over the nuclear one (see e.g. [28]). As mentioned in the previous section, on light targets break-up reactions are dominated by nuclear effects whereas on medium mass targets, both Coulomb and nuclear break-up contribution are important, as well as their interference effect [29]. Similar behavior could also occur for the coupling with the break-up channel.
Very few experiments have been performed of elastic scattering of halo nuclei on medium mass targets. In [11, 27] the elastic scattering ^{6}He+^{64}Zn was measured at 10 and 13.6 MeV and compared with the scattering of the well bound ^{4}He nucleus. From this comparison two main features can be observed: 1) the total reaction cross-section in the ^{6}He case is much larger than in the ^{4}He one ($\approx$ a factor of two); 2) the Coulomb-nuclear interference pattern is reduced. In fig. 2 this comparison at E_{lab}=13.6 MeV is shown.

The large Coulomb dipole break-up probability of ^{6}He and the strong coupling of this process to the elastic scattering could be responsible for the deviation of the ^{6}He scattering from the classical diffraction pattern. This was better investigated in [9] in the study of the scattering induced by a different halo nucleus onto the same ^{64}Zn target: the ^{11}Be nucleus. ^{11}Be is more weakly-bound than ^{6}He and thus has a more extended halo.
In [9, 10], together with the ^{11}Be+^{64}Zn, the ^{10}Be+^{64}Zn elastic scattering was measured as well. As shown in fig. 3, a strong reduction of the elastic cross-section in the Coulomb-nuclear interference region is observed for the ^{11}Be+^{64}Zn collision, much stronger than in the ^{6}He case.

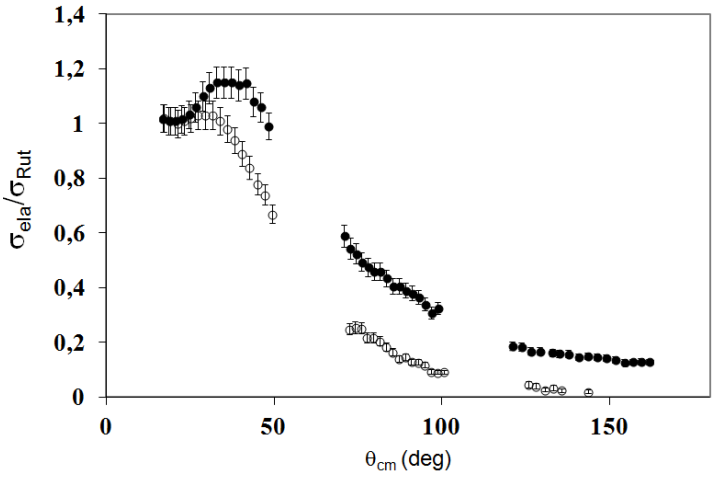

Figure 2. Elastic scattering angular distribution ^{4}He+^{64}Zn (closed symbols) and ^{6}He+^{64}Zn (open symbols) at the same c.m. energy of 12.4 MeV

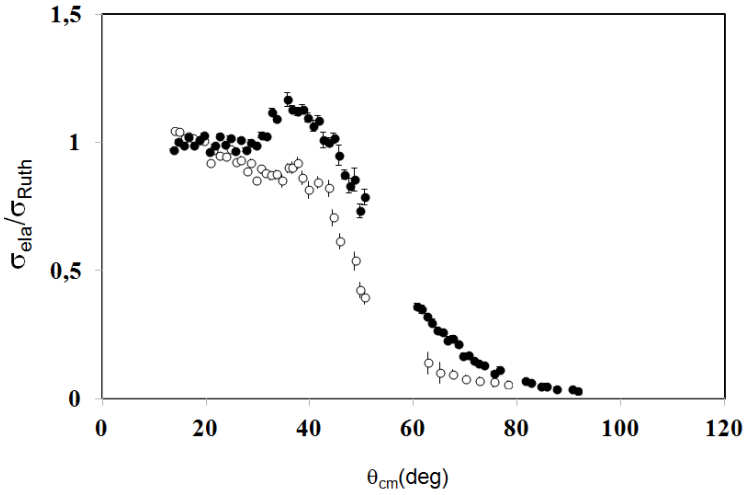

Figure 3. Elastic scattering angular distribution ^{10}Be+^{64}Zn (closed symbols) and ^{11}Be+^{64}Zn (open symbols) at c.m. energy of $\approx$ 24.5 MeV

In the same figure the ^{10}Be+^{64}Zn elastic scattering angular distribution is shown; this angular distribution presents the typical Fresnel diffraction pattern. The TR cross-section in the ^{11}Be case is $\approx$ 2.2 times larger than for the ^{10}Be one.
The OP deduced from the ^{10}Be+^{64}Zn measurement was used as bare potential for the ^{11}Be+^{64}Zn calculations, both for the OM and CDCC calculations.

In the OM analysis two types of DPP potentials were used. 1) A phenomenological DPP having the shape of a Woods-Saxon derivative; 2) a DPP potential derived from the semiclassical theory of Alder and Winter for Coulomb excitation which takes into account the effect of the coupling to the inelastic and break-up channels due to the dipole Coulomb interaction. In the first case a good fit of the data was obtained with a DPP having a very large diffuseness of 3.5 fm, in agreement with what found by [32]. In the second case, adding the DPP to the

bare potential produced a strong reduction of the elastic cross-section in the Coulomb-nuclear interference region; however, this reduction is not sufficient to reproduce the measured data.
The scattering angular distribution for the ^{11}Be case was also compared with CDCC calculations. In these calculations the ^{11}Be+^{64}Zn reaction is treated within an effective three-body model, ^{10}Be+n+^{64}Zn, and coupling to break-up channels is explicitly taken into account. The calculations show that the suppression of the Coulomb-nuclear interference peak observed in the angular distribution is due to a combined effect of Coulomb and nuclear couplings to break-up channels, although they act in very different way. Coulomb coupling gives a large contribution to the break-up cross section and therefore produces an increase of the reaction cross section; nuclear coupling has a large effect on the elastic phase-shift, thus affecting the shape of the elastic angular distribution but not so much the break-up cross section.
The effect of coupling with the 1n and 2n-transfer processes onto the elastic scattering of ^{6}He on a ^{65}Cu target was investigated in [33] using Coupled Reaction Channel (CRC) calculations. A simplified model for the 2n transfer was used in the CRC. These calculations show that the coupling of the 1n-transfer on the elastic process has a small effect; whereas, the effect of 2n-transfer is much stronger and produces a better reproduction of the data. These calculations however present oscillations which are not observed in the experimental data, the authors attributed this difference to an insufficient absorption.

4. Scattering on heavy targets

In scattering on heavy targets, Coulomb interaction should play an even more important role than with lighter targets. The elastic scattering of the ^{6}He and ^{11}Li halo nuclei from heavy targets shows a strong deviation from the standard diffraction behavior, as the one observed for the scattering of ^{11}Be shown in fig. 3. At low energies, below the Coulomb barrier, the usual Coulomb-nuclear interference peak is completely absent [5, 7, 34, 35]. As mentioned in the previous sections, this behavior is evidence of long range absorption. Also the scattering of the ^{6}Li weakly-bound nucleus shows a similar feature on heavy targets but it is much weaker, being rather a reduction of the Coulomb-nuclear interference than a complete absence, similar to what observed in the case of ^{6}He on the medium mass target ^{64}Zn shown in fig. 2. The elastic scattering of ^{6}He+^{208}Pb has been reported in [5, 34, 35, 36] at energies between 14 and 55 MeV. In [35], and in [34] also in the case of scattering of ^{6}He on ^{197}Au, it was investigated whether at low energies, below and around the Coulomb barrier, the Coulomb dipole polarizability (CDP) is totally or partially responsible for the long range absorption. The CDP is fully dependent on the B(E1) energy distribution and accounts for the coupling with break-up states induced by the dipole Coulomb force acting between projectile and target. The data were analysed within the OM framework. In the OM analysis the CDP was introduced via a DPP. It was found that although the CDP produces an important reduction of the elastic cross-section, CDP can only partially account for the long range absorption found. Beside the CDP, an imaginary potential having large diffuseness ($a_i \approx 1.45$ fm) has to be used. This potential accounts for mechanisms such as higher order effects of the Coulomb coupling or nuclear couplings not included in the CDP. The range of the imaginary potential associated to these additional mechanisms, causing long range absorption, is not as large as the range of the CDP.
In [5], CDCC calculations were performed on the ^{6}He+^{208}Pb at E_{lab}=22 MeV. These calculations confirm the importance of the electric dipole operator in order to reproduce the elastic scattering data.
The ^{11}Li+^{208}Pb elastic scattering has been reported in [4]. Very large reduction of the elastic cross-section has been observed as compared with the scattering of the ^{11}Li core, the ^{9}Li nucleus. Four body CDCC calculations were performed which showed that the elastic cross-section is very sensitive to the dipole strength close to the threshold and in particular to a dipole resonance,

still not well established in the literature, whose energy was adjusted at 320 keV above the threshold, to have the best reproduction of the experimental data. These calculations confirm that also for this system the CDP is the main mechanism responsible for the disappearance of the Coulomb-nuclear interference peak and therefore for the long range absorption.

5. Conclusions

Elastic scattering experiments involving halo nuclei, have been performed at several energies and on different targets over a wide range of masses. In this review a selection of the experimental data available in the literature has been reported. Going through all these data some common features can be pinned down. Many of the measured elastic scattering angular distributions of collisions induced by halo nuclei differ completely from the ones induced by the corresponding non-halo isotope. In the halo nuclei case, coupling with the continuum is found to be very important. For collisions on light targets the coupling is mainly with the nuclear break-up and, as the charge of the target increases, coupling with the Coulomb break-up becomes dominant. An effect of the continuum coupling is the feature observed in the low-energy elastic-scattering on medium mass and heavy targets, i.e. the strong reduction, and in some cases the disappearance, of the Coulomb-nuclear interference peak. This effect is the signature for long-range absorption occurring. A consequence of this suppression is a much larger TR cross-section with respect to the one measured in reactions induced by non-halo nuclei.
In the OM analysis, coupling with the break-up is introduced via a complex DPP potential which has a repulsive real part and a surface imaginary part. By assuming an exponential tail for the imaginary surface potential, its diffuseness is directly related to the decay length of the halo wave function. Therefore, from the scattering measurements, direct information on the wave function of the halo nuclei can be deduced.

References

[1] A. Jensen, K. Riisager and D. V. Fedorov 2004 *Rev. Mod. Phys.* **76** 215
[2] R. Raabe et al. 2004 *Nature* **431** 823
[3] V. Scuderi et al. 2011 *Phys.Rev.* C **84** 064604
[4] M. Cubero et al. 2012 *Phys. Rev. Lett.* **109** 262701
[5] L. Acosta et al. 2011 *Phys.Rev.* C **84** 044604
[6] Y. Kucuk, I. Boztosun and N. Keeley 2009 *Phys. Rev.* C **79** 067601
[7] A. M. Moro, K. Rusek, J. M. Arias, J. Gómez-Camacho and M. Rodríguez-Gallardo 2007 *Phys. Rev.* C **75** 064607
[8] T. Matsumoto, T. Egami, K. Ogata, Y. Iseri, M. Kamimura and M. Yahiro 2006 *Phys. Rev.* C **73** 051602(R)
[9] A. Di Pietro et al. 2012 *Phys. Rev.* C **85** 054607
[10] A. Di Pietro et al. 2010 *Phys. Rev. Lett.* **105** 022701
[11] A. Di Pietro et al. 2004 *Phys. Rev.* C **69** 044613
[12] Y. Sakuragi, 1987 *Phys. Rev.* C **35** 2161
[13] N. Keeley et al. 1994 *Nucl. Phys.* A **571** 326
[14] G. R. Stachler 1999 *Phys. Rep.* **199** 147
[15] A. M. M. Maciel et al. 1999 *Phys. Rev.* C **59** 2103
[16] N. N. Deshmukh et al. 2011 *Phys. Rev.* C **83** 024607
[17] M. Zadro et al. 2009 *Phys. Rev.* C **80** 064610
[18] R. C. Johnson and P. J. R. Soper 1970 *Phys. Rev.* C **1** 976
[19] M. Majer et al. 2010 *Eur. Phys. J.* A **43** 153
[20] T. Matsumoto, E. Hiyama, K. Ogata, Y. Iseri, M. Kamimura, S. Chiba, and M. Yahiro 2004 *Phys. Rev.* C **70** 061601(R)
[21] V. Lapoux et al. 2002 *Phys. Rev.* C **66** 034608
[22] K. C. C. Pires et al. 2011 *Phys. Rev.* C **83** 064603
[23] I.J. Thompson, M.A. Nagarajan, J.S. Lilley and M.J. Smithson 1989 *Nucl. Phys.* A **505** 84
[24] M. Milin et al. 2004 *Nucl. Phys.* A **746** 183c
[25] M. Milin et al. 2004 *Nucl. Phys.* A **730** 284

[26] E.A. Benjamim et al. 2007 *Phys. Lett.* B **647** 30
[27] A. Di Pietro et al. 2003 Europhys. Lett **64** 309
[28] N. Fukuda et al. 2004 *Phys. Rev.* C **70** 054606
[29] R. Chatterjee 2007 *Phys. Rev.* C **75** 064604
[30] A. Barioni et al. 2011 *Phys. Rev.* C **84** 014603
[31] J.M.B. Shorto, P.R.S. Gomes, J. Lubian, L.F. Canto, S. Mukherjee, L.C. Chamon 2009 *Phys. Lett.* B **678** 77
[32] A. Bonaccorso and F. Carstoiu 2002 *Nucl. Phys.* A **706** 322
[33] A. Chatterjee et al. 2008 *Phys. Rev. Lett.* **101** 032701
[34] O.R. Kakuee et al. 2006 *Nucl. Phys.* A **765** 294
[35] A.M. Sánchez-Benítez et al. 2008 *Nucl. Phys.* A **803** 30
[36] N.K. Skobelev et al. 1992 *Z. Phys.* A **341** 315